

# Supplemental Material

Elemental analysis was performed by Midwest Microlab.

## High field magnetization

5 Single crystal magnetization data were taken at the Nicholas Kurti Magnetic Field Laboratory, Oxford, using a 45 T pulsed-field magnet with millisecond rise times. The magnetization was measured using a 1500 turn compensated-coil magnetometer made of high purity 50-gauge copper wire. During a magnetic field pulse, the voltage generated in the coil is  $V \propto (-dM/dt)$ , and so numerical integration with respect to time  $t$  can be used to obtain the magnetization  $M$ . The sample was placed inside a PCTFE ampoule, with the magnetic field parallel to the long axis of the crystal. The ampoule can be moved in and out of the 10 magnetometer coil *in situ*, and so accurate magnetization values can be obtained by subtracting empty coil data from that measured with the sample present, under identical conditions.<sup>9</sup> The magnetization measurements were calibrated with the SQUID results to obtain absolute values.

## Muon spin relaxation

15 Zero field (ZF) muon-spin relaxation ( $\mu^+SR$ ) measurements were made at the ISIS facility, STFC Rutherford Appleton Laboratory, UK using the EMU instrument. A powder sample was packed in a 25  $\mu\text{m}$  Ag foil packet and mounted in a  ${}^4\text{He}$  cryostat.

In a  $\mu^+SR$  experiment,<sup>1</sup> spin-polarized positive muons are stopped in a target sample, where the muon usually occupies an interstitial position in the crystal. The observed property in the experiment is the time evolution of the muon spin polarization, the behavior of which depends on the local magnetic field at the muon site. Each muon decays, with an average lifetime of 2.2  $\mu\text{s}$ , into two neutrinos and 20 a positron, the latter particle being emitted preferentially along the instantaneous direction of the muon spin. Recording the time dependence of the positron emission directions therefore allows the determination of the spin-polarization of the ensemble of muons. In our experiments positrons are detected by detectors placed forward (F) and backward (B) of the initial muon polarization direction. Histograms  $N_F(t)$  and  $N_B(t)$  record the number of positrons detected in the two detectors as a function of time following the muon implantation. The quantity of interest is the decay positron asymmetry function, defined as

$$25 A(t) = \frac{N_F(t) - \alpha_{\exp} N_B(t)}{N_F(t) + \alpha_{\exp} N_B(t)},$$

where  $\alpha_{\exp}$  is an experimental calibration constant and  $A(t)$  is proportional to the spin polarization of the muon ensemble.

## Single crystal x-ray diffraction

30 A crystal was glued onto the tip of glass fiber and mounted on a Bruker APEX II 3-circle diffractometer equipped with an APEX II detector. Full data sets were collected at 10, 100, 200, and 298 K. The crystal temperature was maintained through use of an Oxford Cryostream 700 Plus low temperature device for temperatures down to 100 K and a model HFC-1645-LHE Cryocool-LHE (Cryo Industries of America) for the 10 K data collection. The data collection was carried out using MoK $\alpha$  radiation ( $\lambda = 0.71073 \text{ \AA}$ ) with a frame exposure time of 30 seconds and a detector distance of 5.00 cm. Three major sections of frames were collected with 0.30°  $\omega$  scans. 35 Data to a resolution of 0.67  $\text{\AA}$  were considered in the reduction. The raw intensity data were corrected for absorption (SADABS<sup>2</sup>). The structure was solved and refined using SHELXTL.<sup>3</sup> A direct-method solution was calculated, which provided most atomic positions from the E-map. Full-matrix least squares/difference Fourier cycles were performed, which located the remaining atoms. All non-hydrogen atoms were refined with anisotropic displacement parameters. Water hydrogen atoms were located by difference Fourier maps but ultimately fixed in calculated positions. Positions of aromatic H atoms were calculated by employing a “riding” model. Additional details 40 of the data collection are given in Table 1 while selected bond lengths and angles are listed in Table 2.

[1] S.J. Blundell, *Contemp. Phys.*, **1999**, *40*, 175.

[2] G. M. Sheldrick, SADABS, Version 2.03a ed., Bruker AXS, Inc., Madison, WI, USA, **2001**.

[3] G. M. Sheldrick, SHELXTL, Version 6.12 ed., Bruker AXS Inc., Madison, WI, USA, **2001**.

45

**Table 1.** Crystal Data and Structure Refinement of CuF<sub>2</sub>(H<sub>2</sub>O)<sub>2</sub>(3-chloropyridine).

formula	C <sub>5</sub> H <sub>8</sub> ClCuF <sub>2</sub> NO <sub>2</sub>		
$M_w$	251.11		
cryst syst	orthorhombic	monoclinic	
Space group	Pnma	P2 <sub>1</sub> /c	
$a/\text{\AA}$	16.5192(3)	16.4782(3)	6.7670(1)
$b/\text{\AA}$	6.8693(1)	6.8106(1)	7.6416(2)
$c/\text{\AA}$	7.6288(1)	7.6385(2)	16.4281(4)
$\alpha/^\circ$	90	90	90
$\beta/^\circ$	90	90	91.723(1)
$\gamma/^\circ$	90	90	90
$V/\text{\AA}^3$	865.68(2)	857.24(3)	849.12(3)
Z		4	845.3(3)

$D_c/\text{g cm}^{-3}$	1.927	1.946	1.964	1.973
$\mu/\text{mm}^{-1}$	2.822	2.850	2.877	2.890
$F(000)$		500		
$R(\text{int})$	0.0256	0.0174		
Total reflns	11273	11200		
Unique reflns	1560	1531	2826	2811
$I > 2\sigma(I)$	1487	1468	2743	2562
$R(F_o), R_w(F_o^2)$	0.0292, 0.0770	0.0205, 0.0543	0.0205, 0.0580	0.0449, 0.1572
$T/\text{K}$	296(2)	200(2)	100(2)	10(2)

$$^a R(F_o) = \sum |F_o| - |F_c| / \sum |F_o|, R_w(F_o^2) = [\sum w(|F_o^2| - |F_c^2|)^2 / \sum w F_o^2]^{1/2}$$

**Table 2.** Selected bond distances (Å) and angles (°) for CuF<sub>2</sub>(H<sub>2</sub>O)<sub>2</sub>(3-chloropyridine).

	296 K	200 K	100 K	10 K
Bond distances (Å)				
Cu1 – F1	1.8790(13)	1.8834(9)	1.8849(8)	1.887(2)
Cu1 – F2	1.8812(12)	1.8841(9)	1.8871(8)	1.890(2)
Cu1 – N1	2.0617(18)	2.0585(13)	2.0554(11)	2.054(3)
Cu1 – O1	2.0807(12)	2.0783(9)	2.0465(12)	2.030(3)
Cu1 – O2	-	-	2.1110(12)	2.119(3)
Bond angles (°)				
F1 – Cu1 – F2	177.32(6)	177.38(4)	177.47(3)	177.45(9)
O1 – Cu1 – O1(2)	100.42(8)	98.84(5)	97.62(4)	96.83(12)
Hydrogen bonds				
O1 – H1A···F1	1.91(2) Å, 168(2)°	1.93(2) Å, 169(2)°	1.92(2) Å, 163(3)°	1.85(3) Å, 163(5)°
O2 – H2A···F1	-	-	1.90(2) Å, 163(3)°	1.90(3) Å, 159(6)°
O1 – H1B···F2	1.93(2) Å, 169(3)°	1.95(2) Å, 168(2)°	1.92(2) Å, 161(3)°	1.88(3) Å, 164(6)°
O2 – H2B···F2	-	-	1.95(2) Å, 169(3)°	1.88(3) Å, 172(6)°
$\pi$ - $\pi$ interactions (Å)				
ClPy d <sub>centroid-centroid</sub>	3.7181(1)	3.6977(1)	3.7312, 3.6364	3.7597, 3.6028
Cu-Cu separations (Å)				
Cu1-Cu1 (in plane)	5.3509(1)	5.3420(1)	5.2823(3) 5.3848(3)	5.2502(9) 5.4095(9)
Cu1-Cu1 (out of plane)	7.6837(3)	7.6299(2)	7.4409(3) 7.7332(3)	7.348(1) 7.798(1)

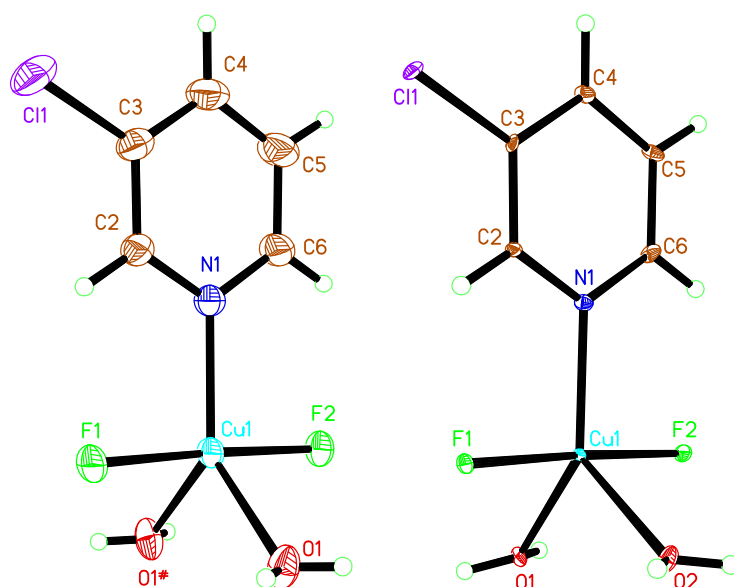


**Fig. S1.** Atomic numbering scheme at 200 K (left) and at 10 K (right). Thermal ellipsoids are drawn at the 50% probability level, with hydrogen atoms drawn as spheres of arbitrary radius. Symmetry code #: x, 1.5-y, z.

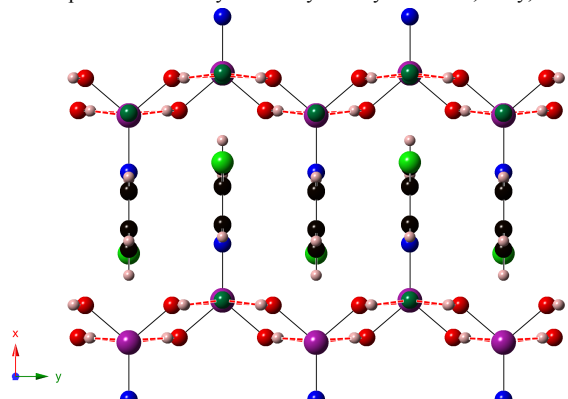


**Fig. S2.** Crystal packing diagrams of  $\text{CuF}_2(\text{H}_2\text{O})_2(3\text{ClPy})$  at 200 K illustrating the 2D hydrogen bonded network and the packing of these layers into a 3D structure through  $\pi-\pi$  interactions of the 3ClPy rings. Color scheme: copper (purple), carbon (black), nitrogen (blue), oxygen (red), chlorine (light green), fluorine (dark green), and hydrogen (pink). Hydrogen bonds are illustrated as dashed red lines.

**Infrared Spectroscopy.** Infrared spectra were measured between 4000 and 750  $\text{cm}^{-1}$  through use of a Bruker Vertex 70 spectrometer equipped with a PIKE Technologies MIRacle™ attenuated total reflectance (ATR) stage.

